

# Challenges in Detecting Wind Turbine Power Loss: The Effects of Blade Erosion, Turbulence and Time Averaging

Tahir H. Malik<sup>1</sup> and Christian Bak<sup>2</sup>

<sup>1</sup>Vattenfall, Amerigo-Vespucci-Platz 2, 20457, Hamburg, Germany

<sup>2</sup>DTU Wind and Energy Systems, Frederiksborgvej 399, 4000 Roskilde, Denmark

**Correspondence:** Tahir H. Malik (tahir.malik@vattenfall.de)

**Abstract.** Establishing a clear correlation between blade leading edge erosion (LEE) and the performance of operational wind turbines is challenging due to the complex interplay of various factors. This study aims to improve the understanding and analysis of real wind turbine measurements by employing aeroelastic simulations to investigate the combined effects of LEE, turbulence intensity ( $TI$ ) and time-interval averaging as a data processing technique and how they obscure the effects of erosion. Importantly, the study does not aim to investigate each contributing factor in detail but seeks to provide insights through selected examples, thereby highlighting how these conditions obscure the detection of blade erosion's effects on power loss. An offshore original equipment manufacturer (OEM) provided aeroelastic model was used to simulate various scenarios. Turbulence intensity was varied for a range of wind speeds and the aerofoil characteristics for the blade were modified to simulate different degrees of erosion, represented by varying levels of roughness. For a given site, findings reveal that even mild simulated erosion can reduce the annual energy production (AEP) by 0.82% at 6%  $TI$ , while more severe erosion leads to a 1.46% decrease. Furthermore, increasing  $TI$  exacerbates these losses, with a 15%  $TI$  causing up to a 2.14% AEP reduction for eroded blades, making it increasingly difficult to distinguish between the effects of blade erosion and turbulence intensity ( $TI$ ) on turbine performance. These effects were most pronounced at sites with lower average wind speeds. Moreover, the interaction between  $TI$  levels and longer time-averaging intervals, which varies with wind speed, can obscure the true magnitude of LEE's impact on short-term power fluctuations. This study demonstrated that 10-minute time-average intervals can significantly mask performance and that analysing unsteady rotor data with shorter time intervals such as 1 second interval are preferable. The work emphasises the importance of considering blade condition's impact in the context of various influencing factors for accurate AEP assessments, performance monitoring and improved wind turbine design for operational wind turbines.

## 1 Introduction

The performance of wind turbines is a multifaceted subject of research, being intricately affected by a multitude of environmental (Wharton and Lundquist (2012)) and operational factors. Wind turbine manufacturers and owners place great focus on this aspect due to its implications for revenue as well as operations and maintenance (O&M). Despite this, accurately identifying and validating performance within operation wind turbines using Supervisory Control and Data Acquisition (SCADA) data remains a major challenge (Ding et al. (2022)). This challenge stems from the complex interplay of factors affecting the

25 turbine's performance (Barthelmie and Jensen (2010)), making it difficult to isolate the effects of individual causes amidst the numerous variables and uncertainties. Consequently, extensive efforts are invested in analysing SCADA data, with the default approach involving the analysis of 10-minute average values of wind speed and power, focusing particularly on power degradation over time. Nevertheless, it is acknowledged that significant uncertainties exist within this 10-minute averaging analysis (Yang et al. (2014)), complicating the detection of LEE effects. In industrial practice, operators typically calculate power curve  
30 loss contributions using static components, employing static tables that include factors such as the thrust coefficient,  $C_t$ , temperature, wind shear, transformer losses and component friction. Yet, quantifying the impact of blade leading edge erosion (LEE) on the power curve for operating turbines remains a challenge. Despite the extensive research on individual factors such as turbulence and other environmental conditions, a comparative analysis of blade erosion's impact relative to effects such as turbulence intensity and time-averaging intervals remains unexplored for operational turbines, which the present study aims to  
35 address.

This study specifically investigates the degradation of power due to LEE. The detrimental effects of LEE or leading edge roughness (LER) on aerofoil characteristics have been extensively documented in wind tunnel experiments (Hansen (2008); Maniaci et al. (2016); Gaudern (2014); Krog Kruse et al. (2021); Bak et al. (2023)). Furthermore, these effects have also been the subject of numerous studies on the impact of erosion on wind turbine annual energy production (AEP) (Bak et al.  
40 (2016); Ehrmann et al. (2017); Kruse (2019); Han et al. (2018); Castorrini et al. (2023)). These studies indicate potentially significant AEP losses of up to 7%. While the impact of blade erosion on AEP is generally smaller than that of wake deficits and some controllers can compensate for degraded lift through pitch adjustments, its subtle effects are nonetheless crucial to quantify. This study employs multibody simulations to capture the interaction between LEE and factors including  $TI$  and data time averaging providing a more quantitative understanding of how these factors obscure performance lossless in SCADA  
45 data, aiming to bridge the gap in understanding. Where, currently, a 1% variance in AEP for Vattenfall, an energy utility, equates to an average daily approximately 380 MWh loss. Although the effects of LEE on aerodynamic performance are easily measurable in controlled environments such as wind tunnels, the question is not whether aerodynamic losses occur; instead, it is why these effects are obscured within the scattered sensor signals of operational wind turbines and how to detect them when a rotor operates in a turbulent flow field with significant wind fluctuations.

50 Analysis of extensive measurement data from wind farms revealed difficulties in obtaining sufficient insight into the influencing mechanisms, a finding supported by studies from Badihi et al. (2022) and Gonzalez et al. (2019). Consequently, simulations of a wind turbine within a wind farm environment were considered more valuable than solely studying SCADA data. The analysis of the simulated data, again, revealed that understanding how turbulence intensity ( $TI$ ) and the effect of averaging unsteady data influenced the results and was crucial for interpreting both measured and simulated data. Furthermore,  
55 turbulence is a well-known atmospheric condition that significantly impacts wind turbine performance (St. Martin et al. (2016); Saint-Drenan et al. (2020); Kim et al. (2021); Cappugi et al. (2021)).

This study aims to investigate selected factors that obscure the detection of erosion-induced power losses in operational wind turbines, an area that has not extensively been examined in previous research. Rather than conducting an exhaustive analysis of all potential contributors, the investigation focuses on providing insights into these obscuring effects through key examples and

60 proposes potential mitigation strategies. While the need for further analysis is acknowledged, the objective is to demonstrate how specific atmospheric conditions and analysis methods complicate the identification of blade erosion’s impact on power loss. A distinctive aspect of this work is the incorporation of a certified model of an operational turbine’s controller into a full aero-servo-elastic simulation loop; which ensures that the response to degraded blades, including pitch adjustments utilising aerodynamic reserves, is captured accurately.

65 In this manner the study aims to improve the understanding and analysis of wind turbine performance measurements, rather than focusing on aerodynamic computations. The goal is to develop more reliable methods for detecting degradation in real-world wind turbine performance. With these aims the study also investigates and compares significant effects, such as turbulence intensity, alongside the impact of degraded aerofoil polar coefficients ( $C_l$  and  $C_d$ ), to uncover why erosion’s effects are not easily detected in SCADA data. The influence of turbulence intensity shall be investigated at the rotor level, expand-  
70 ing upon existing knowledge that primarily focuses on performance at the aerofoil level (e.g., Bak et al. (2008) and Cappugi et al. (2021)). Furthermore, the effects of time interval averaging, traditionally performed using 10-minute intervals, shall be examined.

## 2 Method

This study aims to conduct a fundamental investigation into the impact of turbulence intensity on the aerodynamic perfor-  
75 mance of wind turbine rotors, focusing on the effects of leading-edge erosion. This is achieved using an aeroelastic code that incorporates structural dynamics. Also, the effects of wind shear are briefly investigated. Additionally, the study examines the potential impact of different time-averaging intervals used in operational data analysis on the ability to detect and quantify the effects of leading-edge erosion.

### 2.1 Wind turbine and aeroelastic code

80 The investigation utilises the Blade Element Momentum (BEM) based multi-body aero-servo-elastic tool HAWC2, developed by DTU Wind Denmark. A comprehensive description, usage and implementation of HAWC2 are well-documented in the literature Larsen and Hansen (2007). The certified multibody model used in this study, provided by an OEM, represents a currently operational offshore wind turbine. It is a three-bladed, multi-megawatt, horizontal axis wind turbine with variable speed, pitch regulation and yaw control with a nominal power range of 3 to 4 MW. The Reynolds number,  $Re$ , can be estimated  
85 using the rule of thumb from Bak (2023), which states that  $Re$  is proportional to the rotor radius,  $R$  and falls between  $75,000 \cdot R$  and  $150,000 \cdot R$ . Consequently,  $Re$  is approximately 7 million. Due to intellectual property considerations, specific details about the turbine, such as structural properties and control philosophy, are not disclosed; hence, the power is presented as *normalised power* and is expressed as power relative to the rated power.

While reference wind turbines such as the NREL 5 MW (Jonkman et al. (2009)) or the DTU 10 MW (Bak et al. (2013)) could  
90 have been employed, this study’s close connection to wind farm measurements necessitates incorporating a controller from an actual wind turbine to investigate the unsteady effects. Since relative changes in performance are more critical than absolute

performance, analysing a real wind turbine model is essential. Various parameters, such as damage severity, radial position and the turbine-specific power, impact potential degradation. Therefore, this study is expected to indicate general trends, with specific numerical results varying slightly depending on the actual wind turbine design.

## 95 2.2 Representing leading edge erosion

Blade leading edge erosion was modelled as varying levels of surface roughness, a quantifiable measure of damage severity directly impacting aerodynamic performance and representing a precursor to more significant aerofoil deterioration where voids or cavities may begin to form. The multibody model's blade aerofoil polars for the outer 15% of blade length were modified applying factors to reflect the effects of erosion. The length and location of this applied degradation correspond to field observations of similar blades after approximately two years of operation. Wind tunnel test data from Krog Kruse et al. (2021), which utilised P400 and P40 grit sandpaper to simulate different erosion levels on a NACA 63<sub>3</sub>-418 aerofoil, served as the empirical basis for deriving factors for these modifications. These textures represent the roughness induced by rain droplets impacting the leading edge at high velocities. While the sandpaper provides a simplified model of erosion, it is important to acknowledge that real-world erosion on turbine blades can be influenced by a multitude of factors.

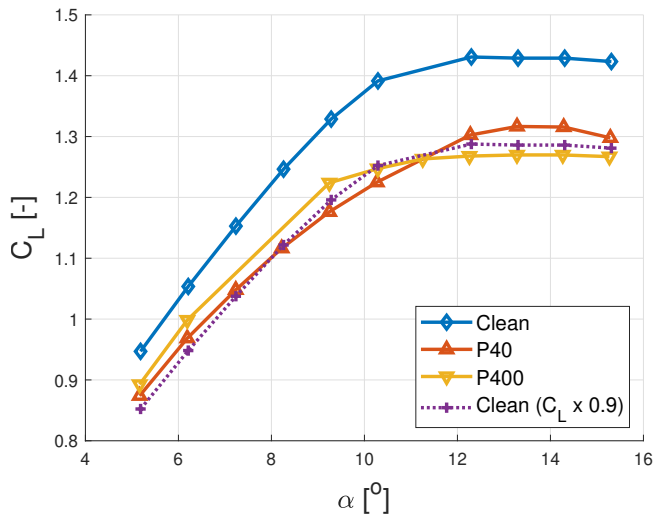


**Figure 1.** Effect of leading-edge erosion on lift coefficient ( $C_L$ ) as a function of angle of attack ( $\alpha$ ). Compares Clean, P40 and P400 blade roughnesses, demonstrating decreased  $C_L$  with increased roughness (measurement data from Krog Kruse et al. (2021))

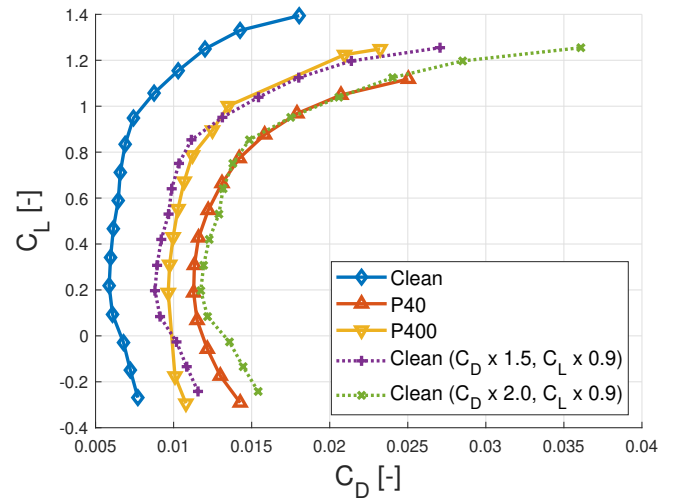


**Figure 2.** Effect of leading-edge erosion on drag coefficient ( $C_D$ ) as a function of lift coefficient ( $C_L$ ). Compares Clean, P40 and P400 blade roughnesses, demonstrating increased  $C_D$  with increased roughness (measurement data from Krog Kruse et al. (2021))

105 A challenge in this work is the lack of access to the aerofoil geometry. Although the aerofoil characteristics are available, they cannot be presented due to intellectual property rights. Therefore, the degradation of the proprietary aerofoil characteristics was modelled by applying relative changes derived from wind tunnel tests on an alternative aerofoil. While Skrzypinski et al. (2014) have proposed a model for altering aerofoil characteristics, this study employs a simplified approach. The tested

alternative aerofoil is not an identical match to that in the multibody model, but this method provides a suitable approximation  
110 for representing the outboard region of eroded turbine blades.

Wind tunnel tests on the alternative aerofoil were conducted at a Reynolds number of  $5 \times 10^6$ . Results for the Clean (no  
sandpaper), P400 (fine, with an average roughness value of 0.035 mm) and P40 (coarse, with an average roughness value  
of 0.415 mm) sandpapers were used. The P40 sandpaper, which has a larger grain size, was chosen to represent a more  
severe erosion state. Figures 1 and 2 illustrate that for both P400 and P40 sandpaper roughnesses, the  $C_{Lmax}$  is reduced  
115 by approximately 10% within a specific range of  $\alpha$  before deep stall. Similarly, the  $C_D$  increases by approximately 50% for  
P400 roughness and 100% for P40 roughness, compared to a clean aerofoil surface. These percentage changes in lift and drag  
coefficients were then applied to approximate the degradation of the proprietary aerofoil polars used in the simulation model.  
For simplicity, the lift polar representing the clean aerofoil was scaled by a factor of 0.9. Additionally, two artificial drag polars  
were created by scaling the drag polar representing the clean aerofoil by factors of 1.5 and 2.0.

120 This approach was deemed acceptable as the multibody simulations were performed over a limited range of angle of at-  
tacks, which is relevant for cases of normal turbine operation, detailed in Section 2.5. These factors were applied between the  
aerofoil's minimum and maximum lift angles of attack. Beyond this range, at high angles of attack (30 degrees), the adjusted  
characteristics were smoothly blended into the original data. The assumption is that at high angles of attack the performance  
is dominated by the flow separation and the resulting pressure distribution, resembling that of a flat plate, thus being less  
125 dependent on the specific surface characteristics. Due to confidentiality, the final modified aerofoil characteristics cannot be  
shown.

### 2.3 Representing wind farm turbulence

The simulations reproduce turbulence conditions typical of operational offshore wind farms. Turbulence data was sourced  
from a meteorological mast located adjacent to an operational offshore wind farm which utilises the same turbine type as the  
130 multibody model.

The turbulence intensity profile at the site, corrected to the turbine's hub height using WindPro EMD International A/S  
(2023), is shown in Figure 3. This comprehensive dataset was derived from six years of 10-minute averaged data and includes  
all wind speeds without directional filtering. It incorporates the effects of wakes from adjacent turbines as well as a wind farm,  
offering a realistic depiction of the first row in a wind farm environment.

135 The mean  $TI$  is 7.3% for the entire period and 6.7% when limited to turbine operational wind speeds - between 4 and 25  
m/s. The  $TI$  distribution is depicted in Figure 4 and together, these figures reveal that although higher turbulence intensities do  
occur, they are relatively rare and primarily occur at lower wind speeds. For sake of convenience in the simulation environment,  
a turbulence intensity of 6% was used to represent mean annual wind farm turbulence with wake free directional filters applied.  
Specific location details of the wind farm and the met mast are omitted due to confidentiality.

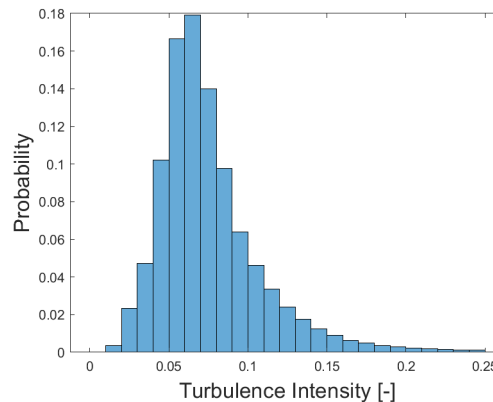
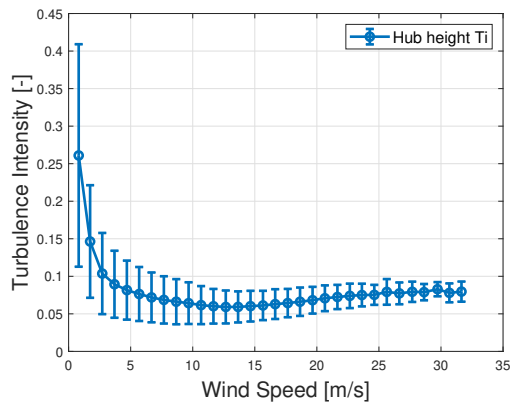


**Figure 3.** Turbulence intensity at the hub height as a function of wind speed. Data obtained from the wind farm’s meteorological mast **Figure 4.** Probability density distribution of turbulence intensity ( $TI$ ) for wind speeds between 4-25 m/s (limited at 25%)

## 140 2.4 Data time averaging

To better understand the potential impact of different data processing techniques on wind and power measurements, this study investigates the effects of varying time-averaging intervals on the detection and quantification of erosion-related power losses. The analysis of wind and power measurements often involves binning and time-averaging. Binning and time-averaging data are forms of data filtering that can both clarify and potentially complicate the interpretation of results. Careful selection of bin sizes is crucial to avoid information loss and potential misinterpretation.

Data time averaging, traditionally over a 10-minute period, is used to smooth turbine signals such as wind speed, power and behaviours such as pitch or torque. These responses are slightly delayed to wind speed, that can fluctuate rapidly. Time averaging can provide a more representative overview of turbine performance and prevailing wind conditions, allowing identification of trends, patterns in data, supported by findings from Abolude and Zhou (2018), Do and Berthaut-Gerentes (2018) and Elliott and Infield that express associated benefits and complexities. While longer intervals simplify data processing and reduce data storage needs, they also risk masking changes in performance and the subtle effects of leading-edge erosion on turbine dynamics (Gonzalez et al. (2017); Gonzalez et al. (2019)).

Importantly, time averaging potentially introduces bias into data analysis. For instance, smoothing out short-term fluctuations in power output can inadvertently alter the perceived shape of the power curve, such as the location of the knee in the power curve. A crucial aspect to consider is the balance between the need to reduce noise in the data and the risk of masking important turbine responses. An excessively short time interval may lead to noisy data, while an interval that is too long risks filtering the turbine’s behaviour too much.

Furthermore, time averaging affects the perceived inertia of the turbine. When power output is averaged over a longer time interval, short-term fluctuations in power output are suppressed, potentially making the turbine appear less responsive to changes in wind speed. If the time interval used for averaging significantly exceeds the characteristic response time of

the turbine, the inertia of the turbine may be underestimated and its ability to respond to changes in wind speed could be overestimated. Conversely, using a time interval that is too short may amplify short-term fluctuations in power output, making data interpretation difficult because the raw data in many cases shall be a swarm of data points. It is therefore important that the specific requirements of the analysis should ultimately dictate the selected averaging time interval.

165 To investigate these effects, this study explores the use of shorter time-averaging intervals to potentially unravel the nuanced effects of leading-edge erosion on turbine performance, which may be masked in traditional 10-minute averages. The challenge lies in selecting an interval that offers sufficient detail without sacrificing clarity, ensuring that critical information about turbine performance and the impact of blade surface conditions is neither lost nor misrepresented. Data from multibody simulations, with a 0.01 second time step, was collected from all wind speed simulation seeds for a given turbulence intensity and blade  
170 profile. Time averaging was then applied to wind speed and turbine sensor variables such as power for time intervals of 0.01, 1, 30, 60, 120, 300 and 600 seconds. Subsequently, the data was averaged into 1 m/s wind speed bins and the turbulence intensity of the original simulation seed was applied to time intervals sliced from it.

## 2.5 Simulation settings and test cases

This study employed a range of simulation cases using HAWC2, a Blade Element Momentum (BEM)-based multi-body aero-  
175 servo-elastic tool, to explore the impact of turbulence intensity and blade erosion on wind turbine performance. Simulations were executed for a range of turbulence intensities for the clean and and two eroded blade profiles. Individual cases were run in 1 m/s increments ranging from 4 to 25 m/s, representing the turbine's cut-in and cut-out wind speeds. Each configuration of wind speed,  $TI$  and blade condition was represented by six individual simulation runs, or seeds, to ensure statistical robustness International Standard. Wind energy generation systems - Part 1: Design requirements. IEC 61400-1 International  
180 Electrotechnical Commission (IEC) (2019).

The turbulence intensity was varied across a broad spectrum including 0%, 4%, 5.5%, 6.0%, 6.5%, 7%, 10%, 15% and 20%, with a focus on values around the observed average annual ambient  $TI$  at an offshore site, along with broader values for comparison. Each simulation was run for 900 seconds, with data from the last 600 seconds used for analysis to ensure steady-state conditions were reached. The time step of the simulations is 0.01 seconds. The wind shear was investigated for  
185 two conditions, including a zero shear value and a power-law profile with an alpha value of 0.14. The air density was fixed at  $1.225 \text{ kg/m}^3$ , representative of sea-level conditions at  $15^\circ\text{C}$ . The Mann turbulence parameter  $\alpha\epsilon^{2/3}$  Mann (1994), energy level was set to its default value of 1.0. For a detailed explanation of specific parameters and settings, refer to the HAWC2 manual Larsen and Hansen (2007) or IEC61400-1 ed. 3 International Electrotechnical Commission (IEC) (2019).

## 3 Results and discussion

190 The simulations conducted in this study have been analysed from multiple perspectives, with the results presented in four distinct sections:

- Effect of shear and blade erosion on power

– Effect of turbulence intensity and blade erosion on power

– Effect on Annual Energy Production

195 – Effect of erosion, time averaging and turbulence on power curve

### 3.1 Effect of shear and blade erosion on power

This section investigates the impact of leading edge erosion on wind turbine power curves under different wind shear conditions using multibody simulations. The simulations were executed at a constant turbulence intensity of 0% to isolate the distinct effects of shear and blade condition. Figure 5 presents normalised power curves for clean blades and those exhibiting P400 and P40 roughness levels, under both zero shear and with imposed wind shear conditions of a power-law profile with an alpha value of 0.14. As expected, the leading-edge roughness reduces the power output across the range of wind speeds.

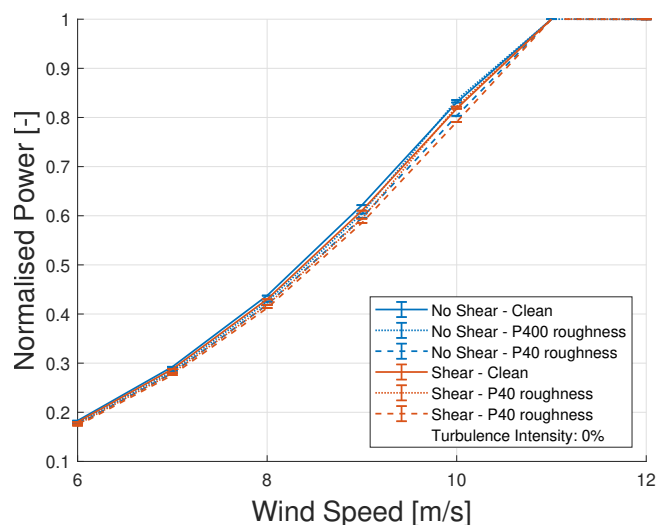


**Figure 5.** Effect of various blade conditions compared to that of shear and no-shear wind condition on the power curve (0%  $TI$ )

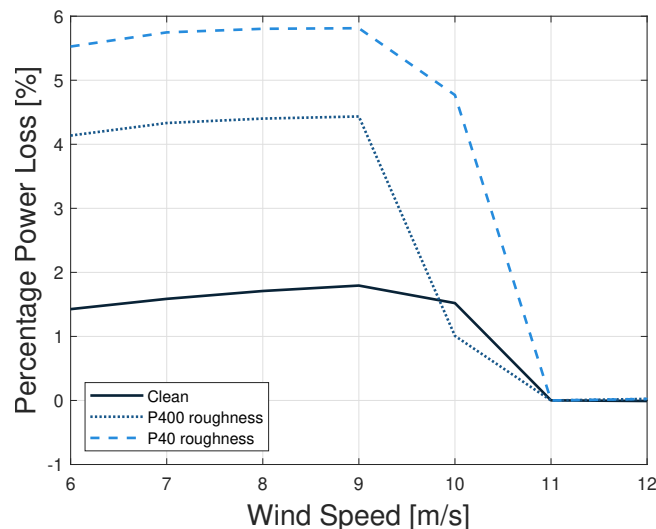


**Figure 6.** Percentage power loss due to shear, referenced against the baseline clean blade without shear, for various blade conditions (0%  $TI$ )

Comparing the no-shear and shear conditions reveals the turbine's sensitivity to shear-induced variations in the wind profile along the rotor span. Under shear conditions, the power curves for both clean and eroded blades exhibit a shift, up to 5.8% for the P40 roughness blade with shear, relative to a clean blade at zero shear conditions, as seen in Figure 6. This demonstrates an adjustment in operational behaviour to account for the velocity gradient imposed by the atmospheric shear and the convoluting effects on power of shear.

Despite these observed shear effects complicating the isolation of variables and highlighting the difficulty of analysing real-world measurement data, this analysis shall focus on investigating turbulence, as it an atmospheric condition whose impact on



performance is typically more substantial than that of wind shear (Saint-Drenan et al. (2020)). Although wind shear remains relevant, the intention is not to investigate each atmospheric condition in detail but rather to illustrate the effects through select examples.

### 3.2 Effect of turbulence intensity and blade erosion on power

#### 3.2.1 Investigation based on the power curves

The normalised, 10-minute averaged power curve of the turbine for various turbulence intensities is shown in Figure 7. Consistent with previous research Saint-Drenan et al. (2020), Wagner et al. (2010), the turbine's power output is significantly influenced by turbulence intensity ( $TI$ ), particularly pronounced within the partial load region of the power curve, which is the operational range between the wind speed where maximum rotational speed is achieved and the wind speed where rated power is reached. The plot includes higher turbulence intensities, such as 20%, to demonstrate the trend in their effect on the power curve. This variance expresses the considerable effect of turbulence intensity on turbine performance.

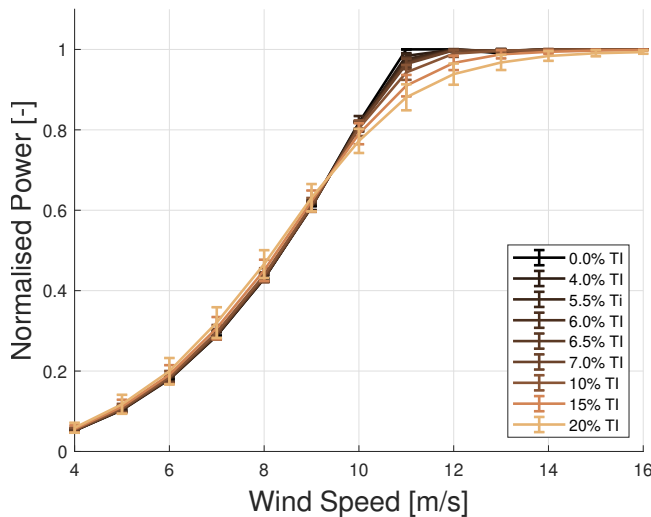


**Figure 7.** Effect of turbulence intensity on the power curve (clean blades)

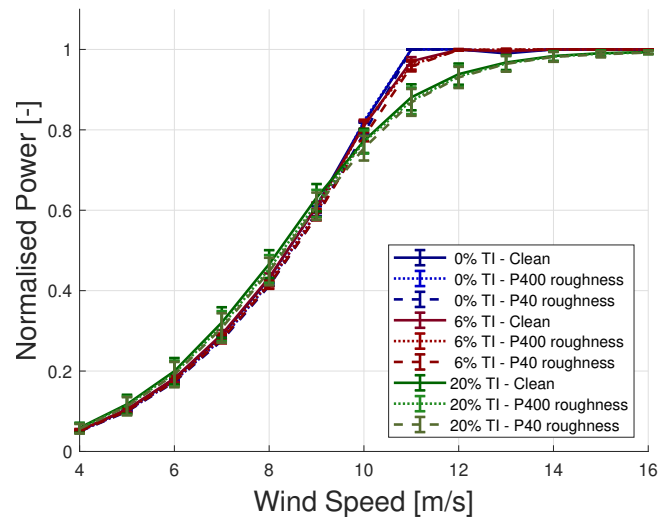


**Figure 8.** Effect of three specific turbulence intensities compared to that of three blade profiles on the power curve

Comparative analysis among Clean, P400, and P40 blade conditions, representing varying degrees of erosion applied on the leading edge of the last 15% of the blade length, are presented in Figure 8. Results are shown for 6% turbulence intensity, representing a typical mean value for offshore sites. The 0% and 20% plots are included for comparison to more outlying conditions, demonstrating a similar trend in power reduction with increasing blade erosion. Similar effect on omitted power curves affirms the consistent detrimental impact of erosion across various  $TI$  conditions.

The figures facilitate a revealing comparison of effects of turbulence relative to erosion. Analysis of the power curve at a specific point, such as the 'knee', reveals that changes in turbulence intensity influence power output are more pronounced than

blade erosion. This is evident in Figure 8: for the clean blade at 11 m/s wind speed, power reduces to approximately 97.0% when  $TI$  increases from 0% to 6% and further to 88.1% at 20%  $TI$ . For eroded blades, these reductions are comparable: 96.2% and 87.2% (P400) and 95.7% and 86.9% (P40).

230 Considering a wind speed of 11 m/s and 6%  $TI$ , erosion causes power losses of approximately 0.9% (P400) and 1.3% (P40) relative to the clean blade. Importantly, the power output's standard deviation at this wind speed is approximately 1.03% (6%  $TI$ ) and 3.23% (20%  $TI$ ). This indicates a major challenge: particularly at higher  $TI$ , the standard deviation exceeds the power loss due to roughness, making it difficult to isolate and detect the effects of erosion on power output based on the power curve alone. Yet, the comparability of values at lower  $TI$  suggests that erosion effects could potentially be detected more readily  
235 under less turbulent conditions.

An interesting observation in Figure 8 is the intersection of power curves around 9.5 m/s. This intersection is caused by a combination of factors. Firstly, the inflection point in the power curve at 9.5 m/s, where the curvature changes, plays a role. Secondly, the averaging effects inherent in calculating power curves from unsteady power output contribute to this phenomenon.

While analysing the changes in power curve shapes provides valuable insights, it offers an incomplete understanding of the  
240 true impact of erosion and turbulence. To accurately assess the overall effect, it is crucial to consider the site-specific wind speed distribution and its influence on the turbine's annual energy production. A more comprehensive analysis is presented in Section 3.3.

### 3.2.2 Investigation relative to a reference power curve

To further investigate how the power curve is influenced by erosion under varying turbulence intensities, this study conducted  
245 a comparative analysis. The change in power relative to a reference Clean profile power curve at 6%  $TI$ , focusing on "P40" roughness, was investigated. The results are shown in Figure 9 as a function of wind speed across a range of turbulence intensities. The delta power curve exhibits a 'kink', a point characterised by a sudden change in gradient, at around 9.5 m/s attributed to the previously discussed effect of time averaging. The most substantial reduction of power due to roughness were identified between 9 and 13 m/s. At lower turbulence intensities, i.e. 7% and below, roughness was found to have an effect in  
250 reducing power. Moreover, for increasing turbulence intensities, the influence of roughness increases dramatically within the same wind speed range.

These findings highlight the non-linear and interdependent relationship between blade roughness and turbulence intensity in their impact on power output. Furthermore, they suggest that both factors must be considered when assessing wind turbine performance, especially within specific wind speed ranges.

### 255 3.2.3 Investigation using power coefficients

The coefficient of power ( $C_p$ ) represents a key metric for evaluating the performance of wind turbines. This study analysed how  $C_p$  varies with wind speed, turbulence intensity and blade roughness. The rationale for investigating  $C_p$  is based on the understanding that turbulence intensity does not inherently alter the efficiency of the wind turbine; rather, it is the combination

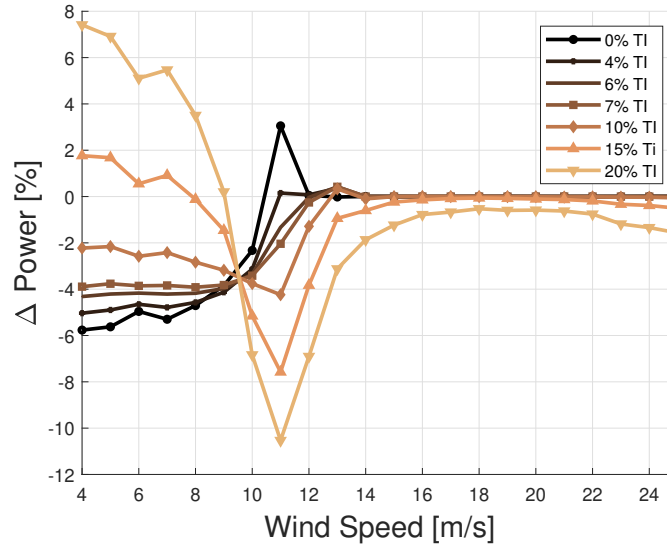


**Figure 9.** P40 profile - Percentage change in power output from the clean baseline as a function of wind speed, showing impact of roughness and *TI* (Baseline: clean profile, 6% *TI*)

of turbulence intensity and the averaging time period that can lead to erroneous conclusions. The power coefficient is calculated  
 260 using the equation:

$$C_p = \frac{P}{0.5 \cdot \rho \cdot V^3 \cdot \pi \cdot R^2} \quad (1)$$

where  $P$  is the power,  $\rho$  is the air density,  $V$  is the wind speed and  $R$  is the rotor radius. Here,  $C_p$  is computed based on the averaged values of wind speed and power. It is important to note that the averaging is performed on wind speed and power separately before calculating  $C_p$ . This investigation also highlights the contrast between steady-state aerodynamic analysis  
 265 with zero turbulence intensity and analysis that includes turbulence intensity. Figure 10 shows the  $C_p$  as a function of wind speed for various turbulence intensities, employing a clean profile blade. The findings indicate that the greatest variation of  $C_p$  is observed at wind speeds below approximately 9 m/s. To evaluate the impact of roughened blade leading edges on  $C_p$ , Figure 11 shows the variation of  $C_p$  for the profiles at 6% turbulence intensity. These results suggest that the impact of both forms of roughness is less pronounced than that of a certain threshold value of turbulence intensity.

270 This investigation analysed multibody simulated data, focusing on the last 10 minutes of each simulation to capture steady-state conditions. Instances where the power coefficient ( $C_p$ ) exceeds or approaches the Betz limit of 0.593 in high turbulence intensity conditions are carefully examined. The exceeding of the Betz limit may be attributed to several factors, including turbine inertia and control dynamics, where the inherent latency in response mechanisms such as pitch and generator torque control results in a temporal mismatch between the turbine's power response and rapid wind speed fluctuations characteristic  
 275 of turbulent environments. This mismatch, particularly when results are time-averaged over a 10-minute window, can yield

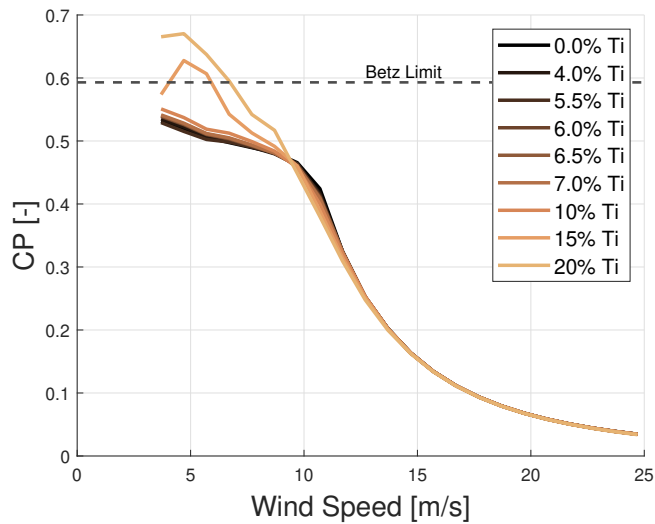


**Figure 10.** Power coefficient as a function of wind speed for a clean profile blade, with various turbulence intensities

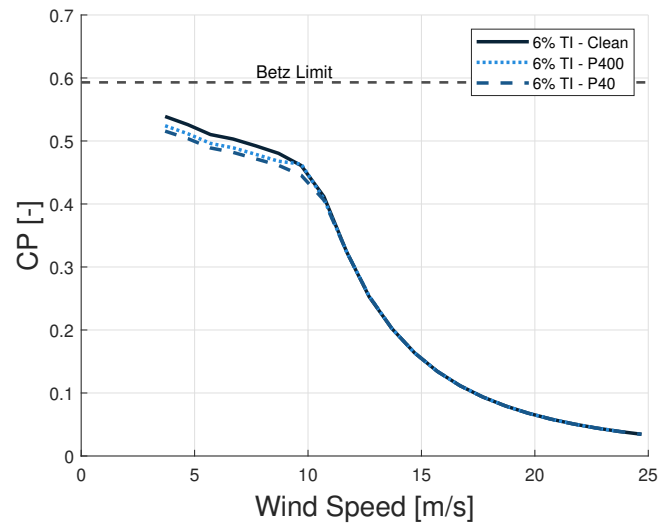


**Figure 11.** Power coefficient as a function of wind speed for three leading edge profiles (6%  $TI$ )

simulated  $C_p$  values that in some conditions surpass the Betz limit. Thus, it is believed that  $C_p$  values exceeding the Betz limit have no physical meaning, rather they are an artefact from the averaging of the wind speed and the rotor performance. Therefore, the analysis can lead to erroneous conclusions.

280 Additionally, the analysis reveals that highly turbulent conditions create localised gusts, temporarily increasing the effective wind speed at segments of the rotor, diverging from steady-state assumptions and causing transient spikes in power output, further exacerbating the mismatch between wind speed and power output. This effect, coupled with the stochastic nature of turbulence that can enhance kinetic energy transfer to the rotor plane and momentarily boost the available wind energy beyond typical averages used in Betz limit calculations. These findings underscore the limitations of steady-state assumptions in accurately capturing the dynamic interactions between wind turbines and complex wind fields. Future research efforts should  
285 focus on refined simulation models and analysis techniques designed to address these limitations.

Figure 12 provides further insight on the combined effects of roughness and turbulence intensity. It depicts  $C_p$  for a limited range of lower turbulence intensities, along with the three blade profiles at 6%  $TI$  for wind speeds up to 11 m/s. The overlap between the  $C_p$ 's for turbulence intensity and roughness suggests that distinguishing between these two effects may be challenging due to the 'masking' effect, particularly in high turbulence conditions. This complicates the interpretation of  
290 aerodynamic performance degradation caused by blade erosion.

### 3.2.4 Summary of the influence of $TI$ and erosion on power

The findings presented herein reinforce the notion that both turbulence and blade erosion exert substantial influences on the wind turbine power output. It has been observed that turbulence profoundly affects the power curve, predominantly in the

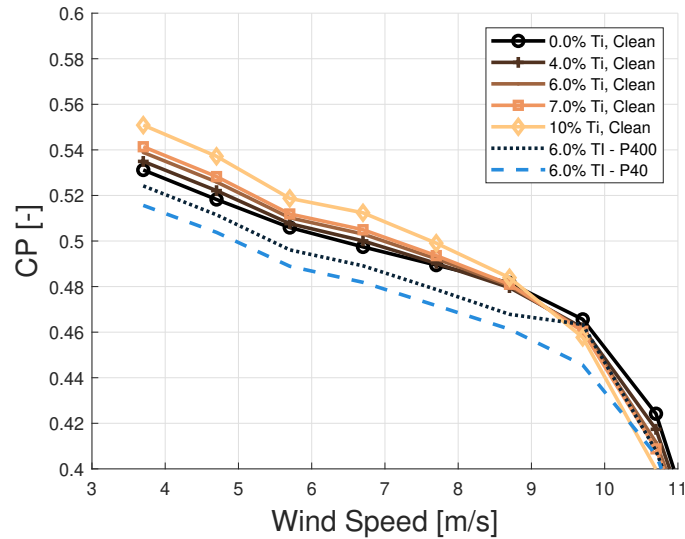


**Figure 12.** Power coefficient as a function of wind speed for a clean profile blade at various turbulence intensities and various leading edge roughness profiles at 6%  $TI$

partial load region. Despite the inherent complexities associated with analysing the performance of the wind turbines under  
 295 turbulent conditions, this study emphasises the significance of incorporating  $TI$  in performance evaluations. This alignment  
 with preceding studies Wagner et al. (2010) and Saint-Drenan et al. (2020) further validates the critical nature of  $TI$  in such  
 analyses.

The examination of delta power shows the detrimental effects blade roughness on wind turbine power output, with the  
 greatest power reduction due to roughness observed at wind speeds between 9 and 13 m/s. This observation is consistent with  
 300 prior research Bak et al. (2020), emphasising the significance of considering roughness effects when assessing wind turbine  
 performance. The study also showed that the impact of roughness on power output is further exacerbated at higher turbulence  
 intensities, suggesting that both turbulence and erosion should be considered in performance assessment.

While the analysis focused on the impact of blade erosion on power, it is important to recognise that erosion could also  
 influence other aspects such as loads and sensor output. These potential impacts warrant further investigation.

### 305 3.3 Annual energy production (AEP) calculation

This section explores the calculation of annual energy production, investigating the impact of both blade erosion and turbulence  
 on wind turbine performance. Analyses included a real-world operational offshore wind farm and hypothetical scenarios at  
 three fictitious sites.

### 3.3.1 AEP for an existing site

310 AEP was calculated for a wind turbine situated in an offshore wind farm operating under mean turbulence intensity of 6%, characterized by a Weibull distribution with a scale parameter  $A = 10.72$ , a shape parameter of  $k = 2.17$ . This corresponds to an average wind speed of 9.49 m/s. The computations expressly exclude the wake effects of upstream wind turbines.

The comparative analysis focused on quantifying the impact of blade erosion and turbulence intensity on AEP by comparing the outcomes for three distinct blade profiles. Table 1 shows the AEP variation for each profile relative to the 6%  $TI$  power  
315 curve of the corresponding profile.

**Table 1.** Change in AEP as a function of  $TI$ . Row 2 shows AEP change relative to “Clean” performance at  $TI=6\%$ ; Row 3 shows AEP change relative to “P400” performance at  $TI=6\%$ ; Row 4 shows AEP change relative to “P40” performance at  $TI=6\%$  with  $V_{ave}=9.49$  m/s

Blade profile	TI [%]							
	0	4	5.5	6	6.5	7	10	15
Clean delta AEP [%]	0.34	0.11	0.03	0	-0.02	-0.04	-0.23	-0.63
P400 delta AEP [%]	0.44	0.11	0.05	0	-0.04	-0.07	-0.29	-0.78
P40 delta AEP [%]	0.51	0.12	0.05	0	-0.04	-0.06	-0.26	-0.70

**Table 2.** Change in AEP as a function of  $TI$  and roughness level: AEP change relative to “Clean” performance at  $TI=6\%$  with  $V_{ave}=9.49$  m/s

Blade profile	TI [%]							
	0	4	5.5	6	6.5	7	10	15
Clean delta AEP [%]	0.34	0.11	0.03	0	-0.02	-0.04	-0.23	-0.63
P400 delta AEP [%]	-0.38	-0.71	-0.77	-0.82	-0.86	-0.89	-1.10	-1.59
P40 delta AEP [%]	-0.96	-1.33	-1.41	-1.46	-1.49	-1.51	-1.71	-2.14

Similarly, Table 2 shows the AEP variation for each profile relative to the Clean blade profile’s 6%  $TI$  power curve. From the results it is clear that even mild simulated erosion, represented by the P400 blade profile, has a significant impact on the turbine’s AEP, with a 0.82% decrease. As erosion progresses, the AEP decreases further to 1.46% for the rougher P40 sandpaper, relative to a Clean blade. Moreover, once a blade is rough, its impact on AEP relative to the Clean blade profile is  
320 significant.

Table 2 also presents turbulence intensities impact on AEP. As turbulence intensity increases, the AEP decreases for all blade profiles. The impact is more significant for the rougher blade profiles, with the P40 sandpaper profile already showing a high decrease in AEP at 2.14% for 15% turbulence intensity.

### 3.3.2 AEP for three fictitious sites with varying wind speeds

325 The investigation extended AEP calculations to three hypothetical sites, each characterised by average wind speeds of 6, 8 and 10 m/s. The subsequent AEP variations for each blade profile, relative to the Clean blade profile's 6% *TI* power curve, are presented in Table 3 for an average wind speed of 6 m/s, Table 4 for an average wind speed of 8 m/s and Table 5 for an average wind speed of 10 m/s. Three different climates are investigated:

- 6 m/s average wind speed:  $k = 2$ ,  $A = 6.8$  m/s (Table 3)
- 330 – 8 m/s average wind speed:  $k = 2$ ,  $A = 9.8$  m/s (Table 4)
- 10 m/s average wind speed:  $k = 2$ ,  $A = 11.3$  m/s (Table 5)

**Table 3.** Change in AEP as a function of *TI* and roughness level: AEP change relative to “Clean” performance at *TI*=6 % with  $V_{ave}$ =6 m/s

Blade profile	<i>TI</i> [%]							
	0	4	5.5	6	6.5	7	10	15
Clean delta AEP [%]	0.16	-0.04	-0.20	0	0.02	0.05	0.25	0.86
P400 delta AEP [%]	-1.20	-1.49	-1.65	-1.47	-1.46	-1.44	-1.28	-0.76
P40 delta AEP [%]	-2.51	-2.84	-3.02	-2.83	-2.82	-2.79	-2.60	-2.00

**Table 4.** Change in AEP as a function of *TI* and roughness level: AEP change relative to “Clean” performance at *TI*=6 % with  $V_{ave}$ =8 m/s

Blade profile	<i>TI</i> [%]							
	0	4	5.5	6	6.5	7	10	15
Clean delta AEP [%]	0.32	0.08	-0.02	0	-0.01	-0.03	-0.13	-0.31
P400 delta AEP [%]	-0.51	-0.85	-0.94	-0.94	-0.97	-1	-1.13	-1.40
P40 delta AEP [%]	-1.39	-1.78	-1.89	-1.88	-1.91	-1.92	-2.03	-2.24

**Table 5.** Change in AEP as a function of *TI* and roughness level: AEP change relative to “Clean” performance at *TI*=6 % with  $V_{ave}$ =10 m/s

Blade profile	<i>TI</i> [%]							
	0	4	5.5	6	6.5	7	10	15
Clean delta AEP [%]	0.30	0.10	0.03	0	-0.02	-0.04	-0.21	-0.61
P400 delta AEP [%]	-0.67	-0.96	-1.02	-1.06	-1.10	-1.13	-1.32	-1.80
P40 delta AEP [%]	-0.84	-1.18	-1.25	-1.29	-1.32	-1.34	-1.52	-1.95

From these results it may be concluded that the impact of turbulence intensity on AEP is more pronounced at lower average wind speeds. This observation is evidenced by the more substantial AEP reductions at lower  $TI$  levels for the P400 and P40 blade profiles, as well as the higher AEP decrease at higher  $TI$  levels for the Clean blade profile, at lower average wind speeds.

335 Simultaneously it is obvious, that the impact of blade erosion on AEP is more significant for lower average wind speeds. This is evident from the larger AEP decrease due to blade erosion for the P400 and P40 blade profiles, as well as the higher AEP decrease for the Clean blade profile, at higher average wind speeds.

The large loss due to erosion for  $V_{ave}=6$  m/s is due to the fact that much of the energy is produced below rated power and that is where erosion has an impact. Erosion has almost no impact at rated power. Smaller losses due to erosion are seen for  
340  $V_{ave}=10$ m/s. The higher the  $TI$ , the more gain when most of the production is made at low wind speeds because the power increases below 9.5 m/s due to the averaging. The higher the  $TI$ , the more loss when most of the production is made at high wind speeds because the power decreases above 9.5 m/s.

Also a trend emerges, suggesting that the comparative effects of blade erosion and turbulence intensity on AEP vary contingent upon the average wind speed and the specific blade profile under consideration. For instance, at an average wind speed  
345 of 6 m/s, blade erosion has a larger impact on AEP than turbulence intensity for all blade profiles. At higher wind speeds, turbulence intensity has a more pronounced impact on AEP, particularly evident in the context of the P40 blade profile.

### 3.3.3 Summary of the effect of $TI$ and erosion on AEP

The investigation into Annual Energy Production encompassed both:

- A specific actual wind climate
- 350 – Three artificial wind climates

For the first AEP calculation the AEP variation for the three blade profiles pertaining to a specific climate with a mean wind speed of 9.49 m/s revealed that even minimal simulated erosion, represented by the P400 blade profile, could precipitate a notable reduction in AEP by 0.82%. As erosion progresses, the AEP decreases further to 1.46% for the coarser P40 sandpaper, relative to a Clean blade. Furthermore, the effect of a blade's roughness on AEP in comparison to the Clean blade profile is  
355 substantial.

The second study additionally examined how three different site specific mean average wind speeds (6, 8 and 10 m/s) affected AEP for the three blade profiles. The findings indicate that at lower wind speeds, the AEP variation caused by turbulence intensity in comparison to a Clean blade profile is more important. This result underlines the importance of considering the level of turbulence intensity there is on AEP in wind farm site selection and design considerations. Notably, the findings from  
360 the hypothetical scenario with the highest wind speed at 10 m/s corresponded well to the first AEP calculation for the specific wind climate.

From the study it was observed that alterations in  $TI$  invariably influence AEP. Such variability introduces complexities in accurately attributing changes in AEP solely to erosion, as fluctuations in  $TI$  could equally account for observed variations.



### 3.4 Influence of erosion, data time averaging and turbulence intensity on the power curve

365 This section examines how blade erosion, data time averaging intervals and turbulence intensity affect wind turbine power curves. Simulations were conducted employing both clean and eroded (P40 roughness) blade profiles.

#### Impact of time averaging intervals from a baseline of 0.01 s time interval at 15% *TI*

Figure 13 illustrates the power as a function of wind speed for different time averaging intervals at a fixed turbulence intensity of 15%. This fixed turbulence intensity was chosen as the baseline to demonstrate the impact of solely time averaging intervals at various wind speeds on the power output. The graph focuses on both the low speed region and knee of the power curve to showcase the varied impact of time averaging across different wind speeds. To quantify these effects Figure 14 presents the percentage change in power relative to the baseline case (Clean profile, 0.01-second interval, fixed 15% *TI*). This visualisation demonstrates the deviations in power output across various averaging intervals, especially at lower wind speeds. By using a fixed turbulence intensity as the baseline, the 15% *TI* example demonstrates significant reductions in observed power with longer averaging intervals, with smaller time intervals showing lower deviations. Notably, the 1-second interval exhibits a more neutral impact on power deviation across the range of wind speeds.

370

375

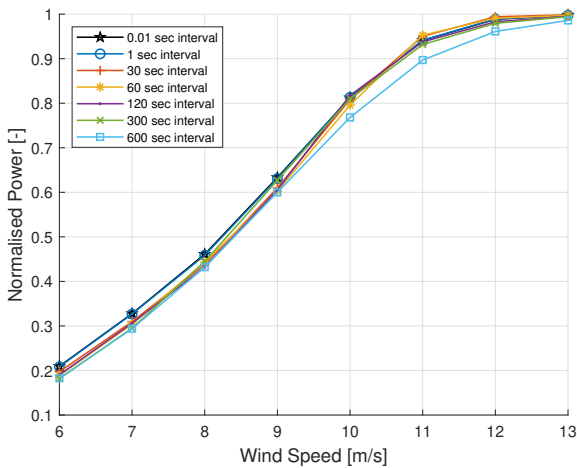


**Figure 13.** Clean profile - Normalised power as a function of wind function of wind speed for multiple time averaging intervals, showing speed for multiple time averaging intervals, showing impact of time impact of time intervals (Baseline: clean profile, 0.01 s interval 15% *TI*)

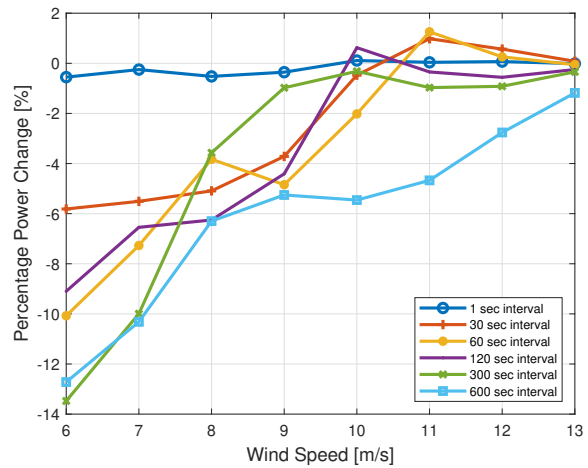


**Figure 14.** Clean profile - Percentage change in power output as a

#### Impact of time averaging intervals from a baseline of 0.01 s time interval with matched *TI*

To further investigate time averaging effects, a baseline case with a clean profile and a 0.01-second interval was used, with the turbulence intensity of the baseline adjusted to match that of the analysed point. The percentage difference in power from the baseline case was calculated for various turbulence intensities for a set of time averaging intervals as illustrated in Figure

380

15, showing the results for a fixed wind speed of 7 m/s, representing the low speed region of the power curve. The data revealed the impact of time intervals as:

- The 1-second time interval showing only a marginal effect
- A trend of increasing power reduction with increasing turbulence intensity
- 385 - Larger time intervals resulting in greater percentage decreases in power

In contrast, Figure 16 shows the results for a fixed wind speed of 11 m/s, representing the knee of the power curve. Here, it is observed:

- Different time intervals exhibiting both increasing and decreasing effects on power output
- Lower time intervals (30 and 60 seconds) pulling the power curve upward
- 390 - 1-second and 120-second intervals having a more neutral effect
- Increasing turbulence intensity having a somewhat linear influence on power change

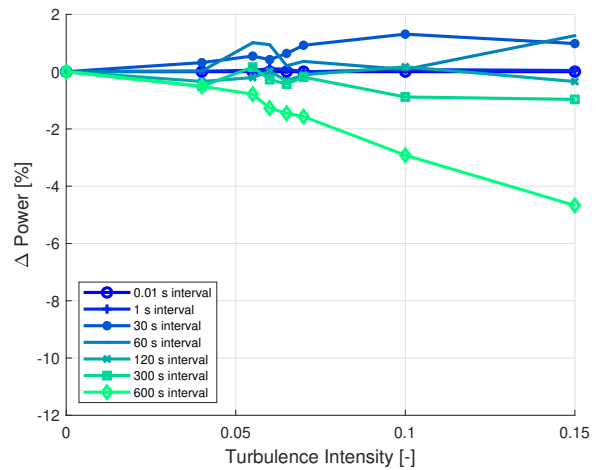
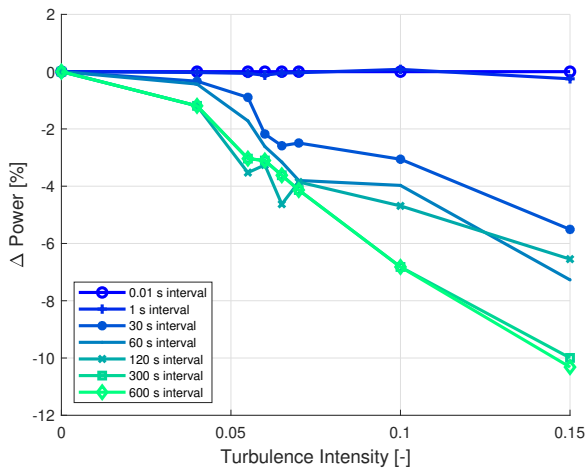


**Figure 15.** 7 m/s, clean profile - Percentage change in power output from the 0.01 second baseline as a function of turbulence intensity, showing impact of time intervals (Baseline: clean profile, 0.01 s interval, matched *TI*) **Figure 16.** 11 m/s, clean profile - Percentage change in power output from the 0.01 second baseline as a function of turbulence intensity, showing impact of time intervals (Baseline: clean profile, 0.01 s interval, matched *TI*)

In both cases, longer time intervals generally show higher delta power than shorter intervals. Still, the magnitude of the change appears larger for the 7 m/s wind speed, indicating a potentially greater impact of time intervals on power output for lower wind speeds. These findings highlight the complex interaction between time averaging intervals at various turbulence

395 intensities for two wind speeds, reinforcing the importance of considering these factors when analysing wind turbine power performance.

**Impact of erosion, time averaging and turbulence from a baseline of a clean blade and fixed 0%  $TI$**

To assess the combined effects of time averaging and turbulence as well as to compare their impacts, initially a Clean blade (i.e. no erosion) profile's impact on power is analysed from a baseline case of a Clean profile at 0.01-second interval and, 400 unlike in the previous two cases, now with a fixed 0%  $TI$ . The impact on power for various time intervals at various turbulence intensities is presented in Figures 17 and 18. Note that erosion is not considered yet. It is observed that:

- Again, the 1 second time interval has a minimal distorting affect for all turbulence intensities and both wind speeds
- At 7 m/s the effect of 15%  $TI$ , is an up to approximately 18% increase in power for the 0.01 and 1 second time intervals
- At 7 m/s looking at the combined effect of time averaging and turbulence, at 15%  $TI$  the effects have a 6.5% power increasing effect for the 600 second time interval
- 405 - At 11 m/s the effect of 15%  $TI$ , is an up to approximately 4.7% decrease in power for the 0.01 and 1 second time intervals
- At 11 m/s looking at the combined effect of time averaging and turbulence, at 15%  $TI$  the effects have a approximately 9% power decreasing effect for the 600 second time interval

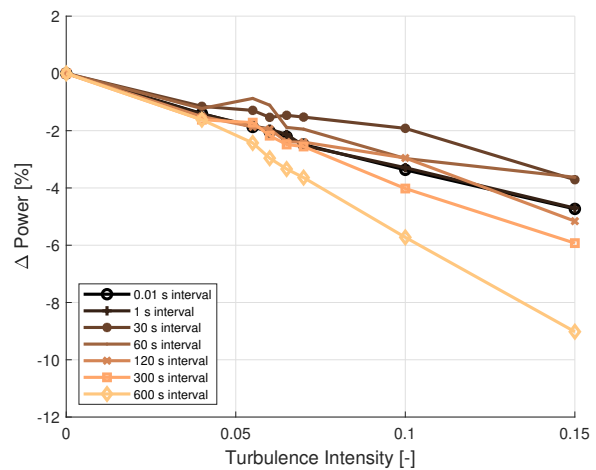
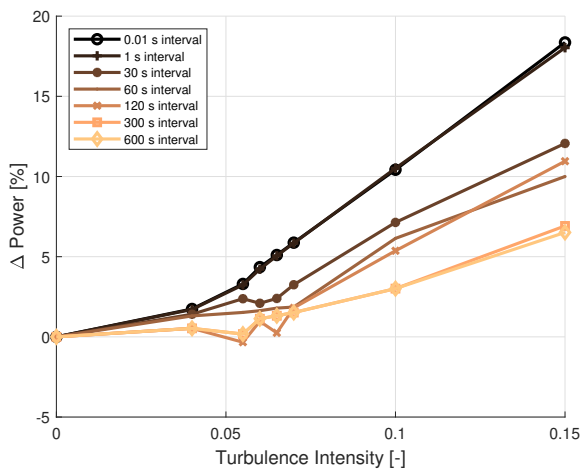


**Figure 17.** 7 m/s, clean profile - Percentage change in power output from the 0.01 second baseline as a function of turbulence intensity, showing impact of time averaging and  $TI$  (Baseline: clean profile, 0.01 s interval, 0%  $TI$ ) **Figure 18.** 11 m/s, clean profile - Percentage change in power output from the 0.01 second baseline as a function of turbulence intensity, showing impact of time averaging and  $TI$  (Baseline: clean profile, 0.01 s interval, 0%  $TI$ )

410 Adding the dimension of blade erosion, which is of particular importance to this study, represented by a P40 roughness, Figures 19 and 20 display results for erosion's influence in addition to time averaging and turbulence. Here the baseline remains the clean blade with 0.01-second interval and a fixed 0% TI. With the addition aspect of erosion it is observed that:

- Yet again, the 1 second time interval has a minimal distorting affect for all turbulence intensities and both wind speeds, despite blade erosion
- 415 - At 7 m/s the erosion, in general, reduces the power across all turbulence intensities comparing to Figure 17, shifting this plot with. For example, an approximately 4% power reduction is observed at 0% turbulence intensity.
- At 11 m/s erosion's effect seems milder impacting power less dramatically than at the lower wind speed

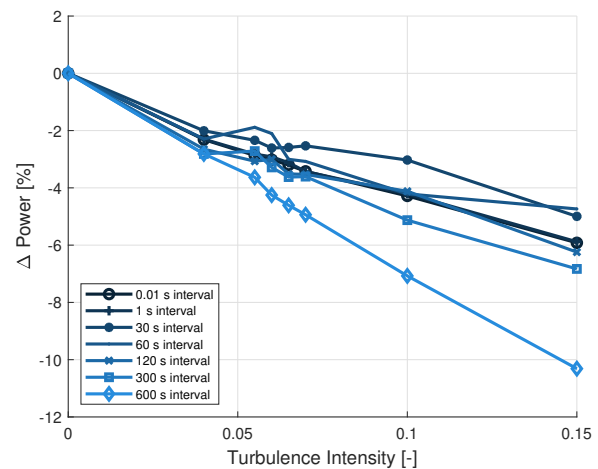
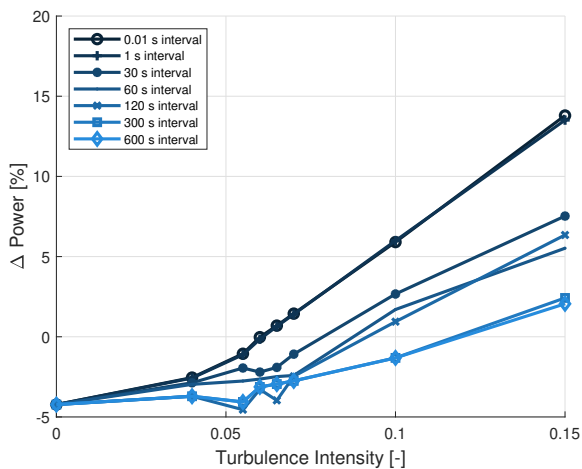


**Figure 19.** 7 m/s, P40 profile - Percentage change in power output from the 0.01 second baseline as a function of turbulence intensity, showing impact of roughness, time averaging and *TI* (Baseline: clean profile, 0.01 s interval, 0% *TI*)

**Figure 20.** 11 m/s, P40 profile - Percentage change in power output from the 0.01 second baseline as a function of turbulence intensity, showing impact of roughness, time averaging and *TI* (Baseline: clean profile, 0.01 s interval, 0% *TI*)

These findings emphasise the importance of choosing appropriate time intervals for data analysis. Short intervals can introduce noise, while long intervals can mask important turbine behaviour. The 1-second interval balances reducing variability without losing significant information. It is crucial to note that the effect of time averaging on power output varies with wind speed and turbulence intensity, precluding a universal correction. For accurate correction, it would be important to use both a turbine simulation model and meteorological mast data for precise *TI* measurements when correcting for time interval averaging influences.

420

### 3.4.1 Summary of the influence of time averaging on power curve

425 The investigation into time averaging effects on power analysis shows the significant impact of time interval selection on the  
resulting power curve. Simulation outcomes revealed that larger time intervals generally lead to a more pronounced decrease  
in power output with increasing turbulence intensity. Despite this, the impact of time averaging on power output varies with  
operational conditions. At lower wind speeds, larger intervals result in a significant power decrease, while at higher wind  
speeds, smaller intervals can increase power output and larger time intervals can decrease it. Notably, a 1-second time interval  
430 maintained a neutral effect across all turbulence intensities.

Comparing the P40 roughness blade to a clean blade at 0% turbulence intensity demonstrated that the blade surface rough-  
ness's impact on power output is less pronounced than time averaging, although both factors significantly affect the power  
curve. Time interval averaging can obscure changes in wind turbine performance due to subtle aerodynamic efficiency mod-  
ifications, such as blade erosion. Short-term changes are harder to detect because averaging smooths out fluctuations in the  
435 turbine's response to changes in wind speed and other variables.

To address this issue, selecting shorter averaging periods is advisable to capture transient variations in turbine performance.  
Although shorter intervals may produce noisier data, this trade-off is necessary for detailed analysis. The study discerned mini-  
mal information loss with 1 second values and generally, shorter periods led to smaller losses. While simulations provide good  
signal control, applying short averaging periods to measured data presents additional challenges due to greater uncertainties in  
440 real-world measurements.

It may be argued that the standard deviation of average values can compensate for the effect of time interval averaging. The  
standard deviation of average values can partially offset time interval averaging effects by estimating lost short-term variability.  
Nevertheless, if the averaging interval exceeds sensor response times significantly, this loss cannot be fully compensated by  
standard deviation calculations.

### 445 3.5 Influence of other factors

Although the current investigation demonstrates the significant impact of blade surface roughness, turbulence intensity and  
time interval averaging on wind turbine power output, it is imperative to acknowledge that additional variables also play crucial  
roles. Among these, atmospheric conditions including shear, that has briefly been demonstrated in this paper to significantly  
influence the performance, as well as temperature, veer, seasonal effects and climate change. Changes in temperature can affect  
450 the viscosity of oils and greases, as well as lead to variations in component losses - for instance those in generators and cables  
- and components stiffness. Other mechanical factors such as, component wear, yaw misalignment, pitch system reliability,  
ageing, operations and maintenance events and increased friction in the drive train, significantly influence turbine performance.  
Moreover, reliable measures of wind speed, necessitating regular calibration of wind speed sensor based on turbine output or  
updates in turbine control software, along with the effects wind speed binning, are pivotal in evaluating turbine performance  
455 accurately. Furthermore, the control of the wind turbine such as generator speed and pitch as a function of wind speed or power,  
potentially influence the outcomes of such analyses.

Although, these aspects were outside the purview of the present study, they warrant further exploration for a comprehensive understanding of their individual and combined impacts on turbine power output. Future research should prioritise a holistic approach to systematically investigate the complex interplay between these factors and their implications for the long-term efficiency and sustainability of wind turbines.

#### 4 Conclusion

This study examines the power and energy losses of multi-megawatt wind turbines caused by erosion-induced degradation of blade leading edges and thereby the aerodynamics. A significant aspect of this work is the use of time-dependent aeroelastic computations to investigate the feasibility of observing the power degradation in real-world measurements. To achieve this, not only were the aerodynamic characteristics degraded, the influence of turbulence intensity and the time-period for averaging data were investigated due to their suspected influence on the analysis.

The investigation reveals that blade roughness significantly affects wind turbine performance; yet, it also demonstrates that turbulence intensity significantly masks this degradation. Based on 10-minute averaging data the impact of turbulence intensity on the power is significant, especially in the partial load region, whereas the impact of blade erosion in this region was less pronounced. Notably, blade roughness can significantly affect power production, particularly at wind speeds between 9 and 13 m/s, i.e. in the transition between the partial load region and rated power.

The study of the power coefficient emphasises the criticality of considering both blade roughness and turbulence intensity when assessing wind turbine performance. It appeared that turbulence intensities greater than approximately 10% make the analysis very challenging. The analysis to determine the power coefficients and encountering values exceeding the Betz limit illustrates this challenge.

Findings of the AEP analysis revealed, for a given site, that even mild simulated erosion can reduce AEP by 0.82% at 6% *TI*, while more severe erosion leads to a 1.46% decrease. Additionally, the study indicates the variable impacts of erosion and turbulence intensity across different wind climates. In climates characterised by lower average wind speeds, the effects of erosion and turbulence intensity on AEP are accentuated compared to those in wind climates with a higher average wind speed. A key finding from this analysis is that turbulence intensities exceeding 10% may introduce significant uncertainties in power performance analysis. Therefore, when feasible, it is recommended to filter out such high turbulence intensity data to ensure more reliable assessment of wind turbine performance.

Furthermore, the exploration of time averaging's influence on power output through simulations across different turbulence intensities and time intervals provides additional insights. The findings indicated that larger time averaging intervals generally result in greater percentage decreases in power and that rising turbulence intensity shows a decrease in power of up approximately 10% for 300 and 600 second intervals at 15% *TI* and 7 m/s wind speed. At the 'knee' of the power curve, at 11 m/s, smaller time intervals of 30 and 60 seconds elevated the power curve, with shorter time intervals of 1 and 120 seconds having a more neutral effect. Longer time intervals of 300 and 600 seconds lowered the power curve by up to approximately -4.5% for the latter interval, at 15% *TI* - although it should be noted that higher turbulence intensities are less likely at increasing

490 wind speeds. Thus, at 11 m/s, different time intervals can have both increasing and decreasing effects on power output. This analysis showed that 10-minutes (600 seconds) average time periods resulted in values significantly different from those based on smaller average time periods. Notably, analysis based on 1-second time periods seems to be neutral to turbulence intensities. Thus, this study indicates that using short time periods results in less influence from turbulence intensity when analysing measurement data.

495 This study improves the identification of degradation in operational wind turbine measurement data, although many uncertainties remain. Future research should broaden the scope to investigate how leading edge roughness, turbulence intensity, wind shear, seasonal effects, yaw misalignment and other factors such as operations and maintenance events collectively influence annual energy production. This research should focus on the long-term implications of these combined effects and could inform the development of optimised maintenance and operational performance monitoring strategies.

500 *Author contributions.* Tahir H. Malik was the primary researcher, responsible for the conception of the study, all experimental work, data collection and analysis and the drafting of the manuscript. Christian Bak, as the PhD supervisor, provided oversight, theoretical support and guidance in refining the research methodology and helped shape the direction of the work.

*Competing interests.* The author Tahir H. Malik has received his PhD funding and is employed by Vattenfall.

505 *Acknowledgements.* We gratefully acknowledge the support of Vattenfall, particularly for financing this study and providing access to vital wind turbine resources. We acknowledge the use of AI language model by OpenAI (2023) for refining the manuscript.

## References

- Abolude, A. T. and Zhou, W.: Assessment and Performance Evaluation of a Wind Turbine Power Output, *Energies*, 11, <https://doi.org/10.3390/en11081992>, 2018.
- 510 Badihi, H., Zhang, Y., Jiang, B., Pillay, P., and Rakheja, S.: A comprehensive review on signal-based and model-based condition monitoring of wind turbines: Fault diagnosis and lifetime prognosis, *Proceedings of the IEEE*, 110, 754–806, 2022.
- Bak, C.: Aerodynamic design of wind turbine rotors, *Advances in wind turbine blade design and materials*, Second edition, by Brøndsted P, Nijssen R, Goutianos S, Woodhead Publishing, Elsevier, 2023.
- Bak, C., Zahle, F., Bitsche, R., Kim, T., Yde, A., Henriksen, L., Hansen, M., Blasques, J., Gaunaa, M., and Natarajan, A.: The DTU 10-MW Reference Wind Turbine, *danish Wind Power Research 2013* ; Conference date: 27-05-2013 Through 28-05-2013, 2013.
- 515 Bak, C., Skrzypiński, W., Gaunaa, M., Villanueva, H., Brønnum, N. F., and Kruse, E. K.: Full scale wind turbine test of vortex generators mounted on the entire blade, in: *Journal of Physics: Conference Series*, vol. 753, p. 022001, IOP Publishing, <https://doi.org/10.1088/1742-6596/753/2/022001>, 2016.
- Bak, C., Forsting, A. M., and Sorensen, N. N.: The influence of leading edge roughness, rotor control and wind climate on the loss in energy production, in: *Journal of Physics: Conference Series*, vol. 1618, p. 052050, IOP Publishing, <https://doi.org/10.1088/1742-6596/1618/5/052050>, 2020.
- 520 Bak, C., Olsen, A., Forsting, A., Bjerger, M., Handberg, M., and Shkalov, H.: Wind tunnel test of airfoil with erosion and leading edge protection, *Journal of Physics: Conference Series*, 2507, 2023.
- Bak, D., Andersen, P., Madsen Aagaard, H., Gaunaa, M., Fuglsang, P., and Bove, S.: Design and verification of airfoils resistant to surface contamination and turbulence intensity, in: *Collection of Technical Papers - AIAA Applied Aerodynamics Conference*, pp. AIAA 2008–7050, American Institute of Aeronautics and Astronautics, 26th Applied Aerodynamics Conference ; Conference date: 18-08-2008 Through 21-08-2008, 2008.
- 525 Barthelmie, R. J. and Jensen, L.: Evaluation of wind farm efficiency and wind turbine wakes at the Nysted offshore wind farm, *Wind Energy*, 13, 573–586, 2010.
- Cappugi, L., Castorrini, A., Bonfiglioli, A., Minisci, E., and Campobasso, M. S.: Machine learning-enabled prediction of wind turbine energy yield losses due to general blade leading edge erosion, *Energy Conversion and Management*, 245, 114567, <https://doi.org/https://doi.org/10.1016/j.enconman.2021.114567>, 2021.
- 530 Castorrini, A., Ortolani, A., and Campobasso, M. S.: Assessing the progression of wind turbine energy yield losses due to blade erosion by resolving damage geometries from lab tests and field observations, *Renewable Energy*, 218, 119256, <https://doi.org/https://doi.org/10.1016/j.renene.2023.119256>, 2023.
- 535 Ding, Y., Barber, S., and Hammer, F.: Data-Driven wind turbine performance assessment and quantification using SCADA data and field measurements, *Frontiers in Energy Research*, 10, 1050342, 2022.
- Do, M.-T. and Berthaut-Gerentes, J.: Optimal time step of SCADA data for the power curve of wind turbine, *Journal of Physics: Conference Series*, 1102, 012025, <https://doi.org/10.1088/1742-6596/1102/1/012025>, 2018.
- Ehrmann, R. S., Wilcox, B., White, E. B., and Maniaci, D. C.: Effect of surface roughness on wind turbine performance, Tech. rep., Sandia National Lab.(SNL-NM), Albuquerque, NM (United States), 2017.
- 540 Elliott, D. and Infield, D.: An assessment of the impact of reduced averaging time on small wind turbine power curves, energy capture predictions and turbulence intensity measurements, *Wind Energy*, 17, 337–342, <https://doi.org/https://doi.org/10.1002/we.1579>.



- EMD International A/S: WindPRO Software for Wind Energy Analysis, <https://www.emd.dk/windpro/>, accessed: 2023-06-01, 2023.
- Gaudern, N.: A practical study of the aerodynamic impact of wind turbine blade leading edge erosion, in: *Journal of Physics: Conference Series*, vol. 524, p. 012031, IOP Publishing, 2014.
- 545 Gonzalez, E., Stephen, B., Infield, D., and Melero, J. J.: On the use of high-frequency SCADA data for improved wind turbine performance monitoring, *Journal of Physics: Conference Series*, 926, 012009, <https://doi.org/10.1088/1742-6596/926/1/012009>, 2017.
- Gonzalez, E., Stephen, B., Infield, D., and Melero, J. J.: Using high-frequency SCADA data for wind turbine performance monitoring: A sensitivity study, *Renewable energy*, 131, 841–853, 2019.
- 550 Han, W., Kim, J., and Kim, B.: Effects of contamination and erosion at the leading edge of blade tip airfoils on the annual energy production of wind turbines, *Renewable energy*, 115, 817–823, 2018.
- Hansen, M. O.: *Aerodynamics of wind turbines*. Earthscan, James & James, 8, 14, 2008.
- International Electrotechnical Commission (IEC): *Wind turbines - Part 1: Wind turbine generators - General requirements*, Tech. rep., Geneva, Switzerland, 2019.
- 555 Jonkman, J., Butterfield, S., Musial, W., and Scott, G.: Definition of a 5-MW Reference Wind Turbine for Offshore System Development, <https://doi.org/10.2172/947422>, 2009.
- Kim, D.-Y., Kim, Y.-H., and Kim, B.-S.: Changes in wind turbine power characteristics and annual energy production due to atmospheric stability, turbulence intensity, and wind shear, *Energy*, 214, 119051, <https://doi.org/https://doi.org/10.1016/j.energy.2020.119051>, 2021.
- Krog Kruse, E., Bak, C., and Olsen, A. S.: Wind tunnel experiments on a NACA 633-418 airfoil with different types of leading edge roughness, *Wind Energy*, 24, 1263–1274, 2021.
- 560 Kruse, E.: *A Method for Quantifying Wind Turbine Leading Edge Roughness and its Influence on Energy Production: LER2AEP*, Phd, DTU Wind Energy, Roskilde, Denmark, (DTU Wind Energy PhD), 2019.
- Larsen, T. J. and Hansen, A. M.: *How 2 HAWC2, the user's manual*, Risø National Laboratory, 2007.
- Maniaci, D., White, E., Wilcox, B., Langel, C., van Dam, C., and Paquette, J.: Experimental Measurement and CFD Model Development of Thick Wind Turbine Airfoils with Leading Edge Erosion, in: *Journal of Physics: Conference Series*, vol. 753, p. 022013, IOP Publishing, <https://doi.org/10.1088/1742-6596/1618/5/052050>, 2016.
- 565 Mann, J.: The spatial structure of neutral atmospheric surface-layer turbulence, *Journal of fluid mechanics*, 273, 141–168, 1994.
- OpenAI: ChatGPT: Optimizing Language Models for Dialogue, <https://openai.com/chatgpt/>, 2023.
- Saint-Drenan, Y.-M., Besseau, R., Jansen, M., Staffell, I., Troccoli, A., Dubus, L., Schmidt, J., Gruber, K., Simões, S. G., and Heier, S.: A parametric model for wind turbine power curves incorporating environmental conditions, *Renewable Energy*, 157, 754–768, 2020.
- 570 Skrzypinski, W., Gaunaa, M., and Bak, C.: The Effect of Mounting Vortex Generators on the DTU 10MW Reference Wind Turbine Blade, vol. 524, IOP Publishing, ISSN 1742-6596, <https://doi.org/10.1088/1742-6596/524/1/012034>, content from this work may be used under the terms of the Creative Commons Attribution 3.0 licence. Any further distribution of this work must maintain attribution to the author(s) and the title of the work, journal citation and DOI. Published under licence by IOP Publishing Ltd; 5th International Conference on The Science of Making Torque from Wind 2014, TORQUE 2014 ; Conference date: 10-06-2014 Through 20-06-2014, 2014.
- 575 St. Martin, C. M., Lundquist, J. K., Clifton, A., Poulos, G. S., and Schreck, S. J.: Wind turbine power production and annual energy production depend on atmospheric stability and turbulence, *Wind Energy Science*, 1, 221–236, <https://doi.org/10.5194/wes-1-221-2016>, 2016.
- Wagner, R., Courtney, M., Larsen, T. J., and Paulsen, U. S.: Simulation of shear and turbulence impact on wind turbine performance, *Danmarks Tekniske Universitet, Risø Nationallaboratoriet for Bæredygtig Energi*, 2010.

- 580 Wharton, S. and Lundquist, J. K.: Atmospheric stability affects wind turbine power collection, *Environmental Research Letters*, 7, 014 005, <https://doi.org/10.1088/1748-9326/7/1/014005>, 2012.
- Yang, W., Tavner, P. J., Crabtree, C. J., Feng, Y., and Qiu, Y.: Wind turbine condition monitoring: technical and commercial challenges, *Wind Energy*, 17, 673–693, 2014.